Molecular Pharmacology Fast Forward. Published on June 12, 2007 as doi:10.1124/mol.107.037101
This article has not been copyedited and formatted. The final version may differ from this version.

Dynamin 2 Regulates Riboflavin Endocytosis in Human Placental Trophoblasts

Amy B. Foraker, Abhijit Ray, Tatiana Claro Da Silva, Lisa M. Bareford, Kathleen M. Hillgren, Thomas D. Schmittgen, and Peter W. Swaan

Department of Pharmaceutical Sciences, School of Pharmacy, University of Maryland, Baltimore, Maryland, USA (A.B.F., A.R., T.C.S., L.M.B., and P.W.S), Drug Disposition, Lilly Research Laboratories, Eli Lilly and Company, Indianapolis, Indiana, USA (K.M.H.), and Division of Pharmaceutics, College of Pharmacy, The Ohio State University, Columbus, Ohio, USA (T.D.S.)

Molecular Pharmacology Fast Forward. Published on June 12, 2007 as DOI: 10.1124/mol.107.037101
This article has not been copyedited and formatted. The final version may differ from this version.

a) Running Title: Riboflavin-Endocytosis Involves Dynamin 2

b) Corresponding Author:

Peter W. Swaan, Ph.D., Department of Pharmaceutical Sciences, University of Maryland, 20 Penn Street, HSF2-621, Baltimore, MD 21201 USA

Tel: (410) 706-0103

Fax: (410) 706-5017

Email: pswaan@rx.umaryland.edu

c) Number of:

Text pages:	35
Figures:	7
References:	45
Words in Abstract:	188
Words in Introduction:	842
Words in Discussion:	1,100

d) Abbreviations:

B_2, riboflavin; RCP, riboflavin carrier protein; RNAi, RNA interference; RME, receptor-mediated endocytosis; CME, clathrin-mediated endocytosis; TGFβ, tumor growth factor β; DNM2, dynamin 2 GTPase; CvME, caveolae-mediated endocytosis; siRNA, short-interfering RNA; DLP1, dynamin-like protein 1; LDH, lactate dehydrogenase; TF, transferrin; CAV1, caveolin 1; CTX, cholera toxin subunit B; PC, Pearson's Correlation.

Molecular Pharmacology Fast Forward. Published on June 12, 2007 as DOI: 10.1124/mol.107.037101
This article has not been copyedited and formatted. The final version may differ from this version.

Abstract

Riboflavin is thoroughly established to be indispensable in a multitude of cellular oxidation-reduction reactions through its conversion to coenzyme forms flavin mononucleotide and flavin adenine dinucleotide. Despite its physiological importance, little is known about specific mechanisms or proteins involved in regulating its cellular entry in humans. Studies involving biochemical modulators and immunological inhibition assays have indirectly revealed that riboflavin internalization and trafficking occurs at least in part through a clathrin-dependent receptor-mediated endocytic process. Here, using a two-tiered strategy involving RNAi (RNA interference) and the over-expression of dominant-negative constructs, we directly show the involvement of this endocytic mechanism through the requirement of the pluripotent endocytic vesicle scission enzyme, dynamin 2 GTPase, in human placental trophoblasts. Similar to the endocytic control ligand, transferrin, riboflavin is shown to exhibit 50% dependence on the functional expression of dynamin 2 for its active cellular entry. Furthermore, this reduced vitamin uptake correlates with > 2-fold higher riboflavin association at the cell surface. In addition, fluorescent ligand endocytosis assays showing colocalization between rhodamine-riboflavin and the immunostained caveolar coat protein, caveolin 1, suggest the active absorption of this important nutrient involves multiple and distinct endocytosis pathways.

Molecular Pharmacology Fast Forward. Published on June 12, 2007 as DOI: 10.1124/mol.107.037101
This article has not been copyedited and formatted. The final version may differ from this version.

Endocytosis is a cellular absorption mechanism that serves as a major route for nutrient and macromolecule entry intrinsic to prokaryotic and eukaryotic cells to promote growth, maintenance and function. Receptor-mediated endocytosis (RME) selectively internalizes specific ligands and commonly depends on clathrin as an accessory coat protein. Clathrin-dependent RME (CME) has been characterized to regulate the absorption and trafficking of a variety of ligands, including transferrin, low density lipoprotein, and tumor growth factor β (TGFβ) (Di Guglielmo et al., 2003; Fielding and Fielding, 1996; van der Ende et al., 1987). In light of the restrictive nature of this uptake process, drug bioavailability can be significantly improved by targeting therapeutics to such absorption mechanisms. In combination with drug stabilizing agents and biochemical modulators to promote targeting to cellular organelles, a substantial increase in membrane permeability of hydrophilic drugs and macromolecules can be achieved, as well as enhanced cellular retention by circumventing efflux transporters (Sheff, 2004). The transferrin pathway, which regulates iron homeostasis, has been a pivotal portal for targeting chemotherapeutics to various tumors that have higher demands for iron over normal cell populations (Daniels et al., 2006). Importantly, the successful design of drug targeting strategies and therapeutic applications can only occur upon thorough molecular characterization of ligand-associated RME systems. The molecular sensors regulating riboflavin (vitamin B_2) homeostasis is a relatively unexplored pathway that has gained recent attention for its proposed importance in fetal development and breast and liver cancer physiology (Rao et al., 2006; Rao et al., 1999; Zempleni et al., 1995).

Vitamin B_2 is an essential nutrient required by oxidation-reduction pathways critical in normal cellular growth, function and maintenance. States of physiological B_2-deficiency have been correlated with clinical manifestations including cardiovascular disease, stunted growth, anemia, and neurodegeneration (Powers, 2003; Powers, 2005). Despite its clinical and physiological value, the cellular mechanism(s) regulating B_2 absorption is poorly defined. Recent

Molecular Pharmacology Fast Forward. Published on June 12, 2007 as DOI: 10.1124/mol.107.037101
This article has not been copyedited and formatted. The final version may differ from this version.

reports suggest one portal of entry for B_2 may involve CME (D'Souza et al., 2006b; Huang et al., 2003; Huang and Swaan, 2000; Huang and Swaan, 2001). These studies demonstrated cytoskeletal dependence and clathrin- and/or Rab5-positive endosomal enrichment of B_2 in placental trophoblasts (BeWo). As both clathrin and Rab5 are endocytic markers of CME, these data suggest B_2 absorption involves CME. Furthermore, analogous to the well-characterized CME ligand, transferrin, a B_2 carrier protein has been proposed to sequester free extracellular B_2 and facilitate its transport to endosomal organelles (Mason et al., 2006). Although such a soluble carrier protein has been characterized in oviparous species (Abrams et al., 1988; Zheng et al., 1988), the identity of a human homolog remains elusive. A major limitation to the B_2-RME model is a lack of direct evidence identifying the functional dependence on critical proteins regulating this nutrient absorption mechanism in humans. Dynamin 2 is a candidate protein regulator of cellular B_2 levels.

Dynamin 2 (DNM2) is a ubiquitously expressed GTPase known to regulate the invagination and constriction of vesicles at the plasma membrane and trans-Golgi domain of mammalian endothelial and epithelial cells (Conner and Schmid, 2003; Hill et al., 2001). It is required by multiple endocytic mechanisms including those pathways dependent on clathrin or caveolin, and consequently it has been described as the "…master regulator of membrane trafficking events at the cell surface." (Conner and Schmid, 2003). Based on prior studies suggesting a B_2-CME mechanism occurring in the placental trophoblast model (D'Souza et al., 2006a; D'Souza et al., 2006b; Huang et al., 2003), we hypothesized that B_2 internalization requires dynamin 2 GTPase. Using the established BeWo system, a two-tiered approach involving RNAi and transient transfections of a GTPase-null (K44A) dynamin 2-expression construct were carried out to elucidate the role of this enzyme in B_2 RME.

To date, the proposed B_2-RME model has been defined exclusively by the involvement of the CME mechanism in humans. However, other distinct RME pathways have been shown to be critical in nutrient absorption. Folate uptake is documented to occur through caveolae-

Molecular Pharmacology Fast Forward. Published on June 12, 2007 as DOI: 10.1124/mol.107.037101
This article has not been copyedited and formatted. The final version may differ from this version.

mediated endocytosis (CvME) in addition to CME (Birn, 2006). Furthermore, prior data that revealed B_2-enrichment to Rab5 GTPase positive-endosomes in human placental trophoblasts and enterocytes (D'Souza et al., 2006b) may reflect a CvME trafficking mechanism. Recent reports have implicated the potential for crosstalk in cargo transport between caveosomes, i.e., an organelle specific to CvME, and Rab5-positive vesicles of CME (Querbes et al., 2006). Thus, it becomes plausible that B_2-RME may involve multiple endocytic pathways. The involvement of CvME in B_2 trafficking in BeWo cells was determined using 3D fluorescence colocalization analyses between internalized rhodamine-labeled B_2 (Phelps et al., 2004) and immunostained caveolin 1 (i.e., a CvME membrane coat protein).

Overall, the objectives of this study were to define the general extent by which B_2 absorption depends on endocytosis as a function of the expression level of the major vesicle scission protein, dynamin 2 GTPase, and evaluate whether B_2-RME involves the CvME pathway in human placental trophoblast cells. Results from this study are the first to directly reveal the dependence of B_2 absorption on dynamin 2 expression in human epithelia, and demonstrates, in addition to CME, the involvement of CvME in intracellular B_2 trafficking.

Molecular Pharmacology Fast Forward. Published on June 12, 2007 as DOI: 10.1124/mol.107.037101
This article has not been copyedited and formatted. The final version may differ from this version.

Materials and Methods

Cell Culture. Human placental trophoblasts (BeWo, passages 205-220) were routinely maintained in a controlled atmosphere at 37 ºC with 5% CO_2 in F-12K culture media (Invitrogen Life Technologies, Carlsbad, CA) supplemented with 10% fetal bovine serum, 1% non-essential amino acids, 100 U/ml penicillin and 100 µg/ml streptomycin. All transfection treatments were tested for cytotoxic effects on cell viability using the lactate dehydrogenase-based CytoTox-ONE™ assay according to manufacturer's instructions (Promega Corp., Madison, WI). All chemicals used in these studies were purchased from Sigma (Sigma-Aldrich Inc., St. Louis, MO) unless stated otherwise.

Duplex SiRNA Transient Transfection. Cells grown to ~ 50-60% confluency were seeded (4.2 x 10^4 cells/cm^2) onto 24-well plates using antibiotic-free F-12K media. Twenty four hours later, cells were briefly washed and pre-incubated in serum-free and antibiotic-free Opti-MEM I media (Invitrogen Life Technologies, Carlsbad, CA) for ~ 2 hours at 37 °C and under 5% CO_2. Following this incubation, cells were transfected in Opti-MEM I media with 20 or 40 nM of 21-mer duplex short-interfering RNA (siRNA) complexed with Lipofectamine™ 2000 (1.5% v/v) according to manufacturer's instructions (Invitrogen Life Technologies, Carlsbad, CA). Cells were incubated with siRNA-lipid complexes at 37 °C and 5% CO_2 for 6 hours, at which time the transfection media was replaced with normal F-12K media lacking antibiotics. Cells were used in experiments 48-72 hours post-transfection. All RNA interference studies involved the use of experimentally validated duplex siRNA targeting the human dynamin 2 gene (DNM2 pool siGenome Smartpool, gene accession no. NM_004945, Dharmacon RNA Technologies, Chicago, IL) and human dynamin-like protein 1 (DLP1, gene accession no. NM_012063, Qiagen®, Cambridge, MA). Targeting siRNA effects were normalized to cells transfected with equivalent amounts of non-targeting duplex siRNA (siControl Non-Targeting siRNA, Dharmacon RNA Technologies, Chicago, IL) and compared to mock (Lipofectamine™ 2000 alone) and untreated cell conditions.

Molecular Pharmacology Fast Forward. Published on June 12, 2007 as DOI: 10.1124/mol.107.037101
This article has not been copyedited and formatted. The final version may differ from this version.

Western Blotting and Chemiluminescence-Based Densitometry. Whole cells transfected 63-68 hours prior with siRNA were harvested and lysed on ice for 20 min in RIPA buffer (10 mM Tris-HCL, pH 7.5, 140 mM NaCl, 1% (v/v) Triton X-100, 1% (w/v) sodium deoxycholate and 0.1% (w/v) SDS) supplemented with a Complete Mini® protease cocktail tablet according to manufacturer's instructions (Roche Diagnostics, Indianapolis, IN). Ten to 15 μg total protein was resolved on 12.5% Tris-HCl Criterion gels (BIO-RAD Laboratories, Hercules, CA), transferred to PVDF membranes, and was immunoblotted using monoclonal antibodies specific to dynamin 2 (0.15 μg/ml final concentration; Calbiochem®, EMD Biosciences Inc., San Diego, CA) or dynamin-like protein 1 (0.25 μg/ml final concentration; BD Pharmingen, San Diego, CA). Primary antibodies were subsequently labeled with horseradish peroxidase-conjugated IgG (1:20,000 (v/v) working dilution; Amersham Biosciences, Little Chalfont Buckinghamshire, England) and detected using the ECL plus system (Amersham Biosciences, Piscataway, NJ). Protein levels were quantitated using chemiluminescence-based densitometry on a chemi-doc universal hood II system (BIO-RAD Laboratories, Hercules, CA) and normalized to the corresponding housekeeping protein expression for either GAPDH (2 μg/ml final concentration; Ambion Inc., Austin, TX) or β-actin (2.4 μg/ml final concentration; Sigma-Aldrich Inc., St Louis, MO).

GTPase-null (K44A) and Wild Type Dynamin 2 Plasmid Transient Transfections and Cotransfections with DNM2 pool siRNA. Characterized wild-type ($DNM2^{WT}$) and dominant-negative ($DNM2^{K44A}$) dynamin 2 expression constructs (both in the mammalian expression vector, pCR3.1, Invitrogen Life Technologies, Carlsbad, CA) were kindly provided by Dr. Mark A. McNiven (Mayo Clinic and Foundation, Rochester, Minnesota) (Cao et al., 1998). Prior to transfections, both plasmids were transformed into DH5-α cells (Invitrogen Life Technologies, Carlsbad, CA), subcultured in Luria broth with ampicillin selection, and purified using the Plasmid Maxi Kit (Qiagen®, Cambridge, MA). Expression vector identities were

Molecular Pharmacology Fast Forward. Published on June 12, 2007 as DOI: 10.1124/mol.107.037101
This article has not been copyedited and formatted. The final version may differ from this version.

confirmed through restriction enzyme digests and sequencing using the following established dynamin 2 primers: forward primer [5'-GAAGAGGGCCATACC-3'] and reverse primer [5'-AGTTGCGGATGGTCTC-3'] (Cao et al., 1998). Cell seeding conditions were maintained as in RNAi studies. Twenty four hours post-seeding, cells were briefly washed and pre-incubated in serum-free and antibiotic-free Opti-MEM I for 2 hours at 37 °C and under 5% CO_2. Cells were transfected using Opti-MEM I with 400 ng plasmid DNA alone or with 40 nM DNM2 pool siRNA and complexed with Lipofectamine™ 2000 (1.5% v/v). Cells were exposed to these transfection complexes for 6 hours at 37 °C and under 5% CO_2. Subsequently, the transfection media was replaced with complete F-12K media devoid of antibiotics. Cells were used in experiments 48-72 hours post-transfection.

Radio-Labeled Ligand Endocytosis Assays. Cells were dosed with either 5 nM [^{3}H]-riboflavin ([^{3}H]-B_2; 41 Ci/mmol; Moravek Biochemicals, Brea, CA) or 10 nM ^{125}I-transferrin (^{125}I-TF; ~ 400 cpm/pmol; iodinated using the IODOGEN® method (Pierce Biotechnology Inc., Rockford, IL) according to established procedures (D'Souza et al., 2006b)) in Hanks' Balanced Salt Solution (pH 7.4) containing 25 mM D-glucose and 10 mM HEPES at 37 ºC for 4 min. Immediately, cells were placed on ice and free ligands (i.e., ligands not bound to cell surface receptors) were removed by washing 3x with ice-cold phosphate buffered saline containing cations Ca^{2+} and Mg^{2+} (PBS, pH 7.4). Plasma membrane bound ligands were then removed by washing cells 2x on ice (5 min/wash) with ice-cold PBS with Ca^{2+} and Mg^{2+} (pH 3.0). Cells were alkaline-lysed (1 N NaOH) at 4 °C for at least 2 hours prior to internalized ligand quantitation. The extent of plasma membrane bound and internalized [^{3}H]-B_2 and ^{125}I-TF was determined using liquid scintillation- or gamma counting, respectively. Both, plasma membrane bound and internalized radio-labeled ligands were normalized to total protein content using the Bradford assay (Bio-Rad Laboratories, Hercules, CA). All [^{3}H]-B_2 uptake data generated at 37 °C was corrected for passively absorbed B_2 that was approximated by performing parallel uptake

Molecular Pharmacology Fast Forward. Published on June 12, 2007 as DOI: 10.1124/mol.107.037101
This article has not been copyedited and formatted. The final version may differ from this version.

assays exclusively at 4 °C. Actively internalized B_2 (i.e., uptake at 37 °C) was defined by subtracting internalized [^{3}H]-B_2 at 4 °C.

Acid wash samples collected after uptake assays represented plasma membrane bound ligands and were compared to internalized samples using the following equations:

$$\%bound = \frac{b_e}{b_e + i_e} \cdot \frac{b_{nt} + i_{nt}}{b_{nt}} \times 100 \quad \text{(Eq. 1)}$$

$$\%absorbed = \frac{i_e}{b_e + i_e} \cdot \frac{b_{nt} + i_{nt}}{i_{nt}} \times 100 \quad \text{(Eq. 2)}$$

The extent of bound ligand was expressed as a percent of the sum of bound (b_e) and absorbed (i_e) ligand under experimental conditions, and was normalized to the percent of bound ligand under non-targeting conditions (b_{nt}) (Eq. 1). Likewise, the extent of absorbed ligand (i_e) was defined as a percent of bound plus internalized ligand under experimental conditions and then was normalized to non-targeting effects (i_{nt}) (Eq. 2).

Fluorescent Ligand Endocytosis Assay and Immunofluorescence Staining. BeWo cells were seeded 3-5 days prior to experiments (5 x 10^3 cells/cm^2) in collagen-coated BD Falcon culture slides (BD Biosciences, Bedford, MA). Following serum starvation for 2 hours, pulse-chase assays with 500 nM rhodamine-riboflavin (Rd-RF) (Phelps et al., 2004), 15 nM AlexaFluor®555-labeled cholera toxin subunit B (CTX, Invitrogen™, Molecular Probes™, Eugene, OR), or 30 nM TAMRA-labeled transferrin (TF, Invitrogen™, Molecular Probes™, Eugene, OR) were carried out according to established methods (D'Souza et al., 2006b; Huang et al., 2003). Cells were dosed with the fluorescent ligands for 2 or 10 min at 37 ˚C and then immediately fixed with 4% paraformaldehyde for 20 min at room temperature. The fixed cells were then permeabilized for 20 min with 0.1% Triton X100 in PBS with Ca^{2+} and Mg^{2+} (pH 7.4). Permeabilized cells were blocked with 3% (w/v) bovine serum albumin in PBS (BSA/PBS, pH 7.4) for 30 min prior to 1 hour immunolabeling for either caveolin 1 with rabbit-anti-CAV1 (1:500

Molecular Pharmacology Fast Forward. Published on June 12, 2007 as DOI: 10.1124/mol.107.037101
This article has not been copyedited and formatted. The final version may differ from this version.

(v/v) final dilution; Sigma, St. Louis, MO) or clathrin (1 μg/ml final concentration; BD Biosciences Pharmingen, San Diego, CA). Cells were thoroughly washed with BSA/PBS and probed with AlexaFluor®405-labeled goat-anti-rabbit- or sheep-anti-mouse IgG ((1:400 (v/v) final dilution; Invitrogen™, Molecular Probes™, Eugene, OR). Fluorescence treatments were preserved using GelMount™ (Biomeda Corp., Foster City, CA) and kept at -20 ˚C until used in fluorescence imaging.

3D Confocal Laser Scanning Microscopy and Colocalization Analysis. Internalized fluorescent ligands and immunostained endocytic marker proteins, caveolin 1 and clathrin, were imaged using a Nikon Eclipse TE2000 E inverted confocal laser scanning microscope (Nikon Instruments Inc., Melville, NY) outfitted with fixed lasers for 405 nm and 543 nm and corresponding emission filters, 450/35 nm and 605/75 nm, respectively. Three dimensional images were acquired using the following settings on Nikon EZ-C1 software (Gold version 2.3, Image Systems Inc., Columbia, MD): Nikon planapochromatic 60xA oil objective (1.4 numerical aperture), 3.6 μs scan dwell time, 512 x 512 pixel size resolution, 0.30 μm z-step, and a 150 μm detector pinhole. Raw images were iteratively deconvolved using a calculated point spread function for individual channels and corrected for background noise using a combination of median filtration and setting threshold levels just above negative control treatments with either a non-reactive rhodamine derivative (carboxytetramethylrhodamine-4-amine, a byproduct of the rhodamine-riboflavin conjugation reaction (Phelps et al., 2004)) or the secondary AlexFluor®405 antibody alone. Restored images were analyzed for 3D colocalized fluorescence between ligands and endosome markers using Volocity, version 3.6.1 (Improvision Inc., Lexington, MA). The extent of colocalization between ligands and endocytic markers was determined by calculating the percent of total overlap volume (μm^3) over the corresponding total ligand volume.

Statistics. One-way ANOVA with Dunnett's or Neuman-Keuls multiple comparison tests were used to define statistical significance between the effects of targeting siRNA or wild type

Molecular Pharmacology Fast Forward. Published on June 12, 2007 as DOI: 10.1124/mol.107.037101
This article has not been copyedited and formatted. The final version may differ from this version.

and dominant negative dynamin 2 construct treatments and control conditions (i.e., non-targeting siRNA, empty vector, mock, and untreated treatments) on ligand trafficking. Statistical significance between the effects of targeting siRNA and controls (i.e. non-targeting siRNA or untreated conditions) on dynamin protein levels was defined using the non-parametric Student's *t*-test. True fluorescence colocalization between channels for fluorescent ligands and immunostained endocytic markers was defined using the Pearson's correlation (Manders et al., 1993).

Molecular Pharmacology Fast Forward. Published on June 12, 2007 as DOI: 10.1124/mol.107.037101
This article has not been copyedited and formatted. The final version may differ from this version.

Results

SiRNA Targeting Dynamin 2 or Dynamin-Like Protein 1 Results in Specific Protein Knockdown While Maintaining Cell Viability. In addition to the use of non-targeting siRNA treatments and in order to clearly validate siRNA specificity, all RNAi transient transfection studies included external control conditions involving siRNA targeting a dynamin homolog, dynamin-like protein 1 (DLP1). Like DNM2, DLP1 is a member of the dynamin superfamily (Praefcke and McMahon, 2004), and shares ~ 36% sequence homology to DNM2. In contrast to DNM2, DLP1 is not involved in endocytic vesicle scission events, and has been largely characterized to function in the morphological maintenance of peroxisomes and mitochondria (Praefcke and McMahon, 2004). Based on the current understanding of DLP1, we hypothesized this protein is not involved in the endocytosis of B_2.

BeWo cells were transiently transfected with 20 or 40 nM targeting siRNA for dynamin 2 GTPase (DNM2 pool) or DLP1. Cells were harvested 63-68 hours after initiating siRNA transfections and analyzed for target dynamin knockdown using immunoblotting and chemiluminescence-based densitometry. Upon normalization to housekeeping protein levels, the extent of dynamin expression was defined as a percentage of detected dynamin in cells treated exclusively with non-targeting siRNA (N). Parallel cell populations that were treated with the lipid transfection reagent (Mock) or untreated cells served as additional negative controls. Twenty and 40 nM DNM2 pool siRNA treatments substantially reduced dynamin 2 (100 kDa) expression levels to a similar extent (Fig. 1A). However, 20 and 40 nM DLP1 siRNA specifically knocked down DLP1 protein (83 kDa) expression in a dose-dependent manner (Fig. 1B). The lack of a dose-dependent effect on dynamin 2 expression with the DNM2 pool siRNA conditions may reflect a more robust siRNA formulation, which involves the co-administration of 4 different duplex siRNAs targeting different regions of the DNM2 mRNA. Quantitative densitometry revealed 40 nM DNM2 pool siRNA treatments led to ~ 78% (21.95 ± 7.03% N) and ~ 82% lower

Molecular Pharmacology Fast Forward. Published on June 12, 2007 as DOI: 10.1124/mol.107.037101
This article has not been copyedited and formatted. The final version may differ from this version.

dynamin 2 GTPase levels compared to non-targeting siRNA treated and untreated cells, respectively (Fig. 1C). To a similar extent, 40 nM DLP1 siRNA conditions resulted in ~ 62% (37.65 ± 11.13% N) and ~ 63% lower DLP1 protein levels compared to non-targeting siRNA and untreated conditions, respectively (Fig. 1D). Neither of the dynamin siRNA treatments revealed significant off-target effects at the protein level. Furthermore, dynamin protein levels were shown to be similar between non-targeting siRNA treatments and untreated cell conditions. This data suggests the negative control siRNA transfection effects are not significantly altering target protein levels, and serves as a valid reference for targeting siRNA data normalization.

Cell viability under all transfection treatments was examined for potential cytotoxic effects as a function of lactate dehydrogenase (LDH) release. Cells treated with the various siRNA conditions, plasmid transfections, and mock transfected cell populations were tested for LDH release 48 hours post-transfection. No significant cell death was revealed for any of the transfection treatments, and cell viability for these conditions was at or near those measured for untreated BeWo cells (data not shown). Taken together, these data indicate that siRNA treatments at the 40 nM dose specifically knock down target dynamin proteins without compromising cell viability, and justify the RNAi methodology.

Silenced Dynamin 2 Results in a Significant Reduction in [^{3}H]-B_2 Internalization at Physiological Temperatures. It has been well established that B_2 gains entry into human epithelial cells via multiple mechanisms, including a passive diffusion component that appears to dominate at oversupplemented riboflavin levels and an active component that has been reported to coincide with μM B_2 concentrations (Foraker et al., 2003). One of the salient features defining an active absorption mechanism is temperature dependence. Saturable absorption kinetics have been consistently shown to correlate with physiological temperatures (~ 37 ºC), while low temperatures (~ 4 ºC) generate linear absorption profiles reflecting passive diffusion (Said and Ma, 1994). In fact, B_2 transport has been reported to be dependent on temperature in divergent cell models (Huang and Swaan, 2001; Said and Ma, 1994). However, temperature

Molecular Pharmacology Fast Forward. Published on June 12, 2007 as DOI: 10.1124/mol.107.037101
This article has not been copyedited and formatted. The final version may differ from this version.

dependence alone does not discriminate between a carrier/transporter and receptor-mediated endocytic process. Therefore, in order to differentiate between such active uptake mechanisms, the standardized RNAi methods involving siRNA-induced silencing of the conserved endocytic protein, dynamin 2 GTPase, in combination with the effects of temperature change on B_2 absorption were investigated. To date, the human placental trophoblast cell model (BeWo) has been shown to express high affinity for riboflavin (~ 2 nM) (Huang and Swaan, 2001), and such nM affinities further suggest the involvement of RME in this vitamin's cellular uptake. Combined with prior reports suggesting a B_2-specific RME absorption process (D'Souza et al., 2006a; D'Souza et al., 2006b; Huang et al., 2003; Huang and Swaan, 2001), these data validate the utility of the BeWo cell model to characterize the B_2-specific RME pathway(s). BeWo cells transfected with 40 nM targeting or non-targeting siRNA 63-72 hours prior were used in endocytosis assays. Transiently transfected cells were dosed with 5 nM [^{3}H]-B_2 for 4 min at 4 ˚C or at 37 ˚C. The 4 min internalization period was chosen for all endocytic assays as this is the characterized time interval coinciding with the logarithmic uptake phase typical of RME mechanisms (Schmid, 2004). Passively diffusing riboflavin was defined by vitamin uptake detected at 4 ˚C. Actively internalized B_2 was determined by the amount of B_2 absorbed at 37 ˚C minus that absorbed at 4 ˚C. For the remainder of this report, all actively internalized B_2 data shown represents the active absorption component, exclusively. In contrast to all other transfection conditions, DNM2 pool siRNA-induced silencing of dynamin 2 GTPase resulted in a significant reduction of 50% (i.e., 0.18 ± 0.11 SD and 0.37 ± 0.09 SD pmol/mg prot/4 min for DNM2 pool siRNA treated and untreated cells, respectively) in actively absorbed B_2 compared to internalized B_2 in untreated cell populations (Fig. 2A). As expected, passively diffusing B_2 (i.e., uptake at 4 ˚C) was unaffected by all transfection conditions (Fig. 2B). Collectively, these results further substantiate the involvement of classical RME machinery, i.e., dynamin 2 GTPase, in regulating active absorption of B_2 in placental trophoblasts.

Molecular Pharmacology Fast Forward. Published on June 12, 2007 as DOI: 10.1124/mol.107.037101
This article has not been copyedited and formatted. The final version may differ from this version.

Iodinated transferrin (^{125}I-TF or TF) was chosen to serve as a positive control ligand in all endocytosis assays. Transferrin is an iron carrier protein that has been thoroughly characterized to be internalized via the classical clathrin dependent endocytic pathway, which is known to be regulated by dynamin 2 expression in A431 cells (Lamaze et al., 1993). Thus, transferrin uptake is expected to be significantly inhibited under DNM2 pool siRNA treatments. BeWo cells were transiently transfected with 40 nM targeting or non-targeting siRNA 63-72 hours prior to performing uptake assays. Cells were then dosed with either 5 nM [^{3}H]-B_2 or 10 nM ^{125}I-TF for 4 min at 37 ˚C. The effects of all treatments, including mock and untreated conditions, on ligand absorption were defined as the percentage of non-targeting siRNA effects. Interestingly, both actively internalized B_2 and TF were significantly reduced to a similar extent exclusively under silenced dynamin 2 states. Riboflavin internalization reduced by ~ 40% (59.45 ± 24.70% SD of N, Fig. 3A) and transferrin absorption reduced by ~ 30% (69.64 ± 4.27% SD of N, Fig. 3B). The attenuation in transferrin uptake seen exclusively with DNM2 pool siRNA treated cells is in agreement with literature reports revealing this ligand's dependence on CME and dynamin 2 expression (Cao et al., 2003), and further validates the specificity of the RNAi methodology. A similar effect on B_2 absorption under these same conditions further corroborates prior evidence suggesting this vitamin is internalized via CME (D'Souza et al., 2006a; D'Souza et al., 2006b; Huang et al., 2003; Huang and Swaan, 2000; Huang and Swaan, 2001; Mason et al., 2006; Phelps et al., 2004). Furthermore, the reduced absorption of B_2 (40%) directly correlated with ~ 80% reduced protein expression for DNM2 (Fig. 1C). Thus, we can approximate that at least 50% of the active component regulating B_2 absorption in human placental trophoblasts requires dynamin 2-dependent RME events.

B_2 Enrichment at the Plasma Membrane Doubles Under Silenced Dynamin 2 States. Dynamin 2 GTPase has been extensively characterized to function as a critical gate keeper of intracellular trafficking in that it is required in endosomal vesicle formation and release from the plasma and Golgi membranes (McNiven et al., 2000). Without functional dynamin 2,

Molecular Pharmacology Fast Forward. Published on June 12, 2007 as DOI: 10.1124/mol.107.037101
This article has not been copyedited and formatted. The final version may differ from this version.

RME mechanisms such as clathrin-dependent RME are prevented from forming endosomal vesicles and thus unable to transport their cargo from the plasma membrane or Golgi domain to various other destinations in the cell. Instead, ligand-bound receptors are restricted to these membranes. In light of the evidence of attenuated uptake for both B_2 and TF shown exclusively under silenced dynamin 2 treatments, we would expect a concomitant increase in ligand concentrations bound at the cell surface. To test this hypothesis we analyzed the extent of plasma membrane bound ligand detected after the 4 min uptake period, and compared these data to the extent of internalized ligand.

Membrane bound and internalized ligands detected under the varying 40 nM siRNA treatments were normalized to non-targeting siRNA effects, and were expressed using equations 1 and 2 defined under materials and methods. As expected, DNM2 pool siRNA treatments led to a more pronounced increase in the extent of bound B_2 at the plasma membrane, which coincided with a concomitant decease in its internalization. Likewise, plasma membrane TF localization was enhanced under silenced dynamin 2 conditions. Specifically, under silenced dynamin 2 states, plasma membrane bound B_2 was shown to be ~ 150% higher than bound ligand revealed for untreated cells (Fig. 4A). In addition, internalized B_2 reduced by ~ 40% compared to untreated conditions. Although to a lesser extent than that shown for B_2, membrane bound TF detected for cells treated with DNM2 pool siRNA increased ~ 110% over bound ligand detected in untreated cell populations (Fig. 4B). Furthermore, TF uptake reduced ~ 30% under attenuated dynamin 2 levels as compared to untreated cells. Both B_2 and TF showed substantial localization at the plasma membrane with dynamin 2 silenced treatments when compared to the corresponding internalized ligand data. Both ligands revealed nearly 200% higher enrichment at the plasma membrane than within the cell. In addition, when the extent of bound over the extent of internalized ligand was expressed as a ratio, both B_2 and TF were shown to be 3.1- and 2.0-fold higher than that defined for untreated conditions, respectively (Fig. 4C and D).

Molecular Pharmacology Fast Forward. Published on June 12, 2007 as DOI: 10.1124/mol.107.037101
This article has not been copyedited and formatted. The final version may differ from this version.

B_2 is Substantially Enriched at the Membrane Surface in Cells Transiently Transfected with GTPase-Null Dynamin 2 (K44A). A common approach in corroborating RNAi data involves the use of wild-type and dominant-negative expression vectors. We obtained fully characterized wild-type dynamin 2 ($DNM2^{WT}$) and GTPase-null dynamin 2 ($DNM2^{K44A}$) expression constructs, the latter of which is unable to hydrolyze GTP and thus unable to pinch off nascently formed endocytic vesicles at the plasma membrane (Cao et al., 1998). BeWo cells were transiently transfected with 400 ng of plasmid DNA (wild-type dynamin 2 ($DNM2^{WT}$), GTPase-null dynamin 2 ($DNM2^{K44A}$), or the empty expression vector) in the presence or absence of 40 nM DNM2 pool siRNA. Cells were dosed with either 5 nM [^{3}H]-B_2 or 10 nM ^{125}I-TF for 4 min. When both B_2 and TF results were expressed as a ratio of plasma membrane bound ligand over internalized ligand, a strikingly similar trend was revealed (Fig. 5). Both ligands were shown to be largely localized at the cell membrane, as opposed to the intracellular environment, under GTPase-null dynamin 2 alone and cotransfection conditions (i.e., $DNM2^{K44A}$ or DNM2 siRNA + $DNM2^{K44A}$, respectively). Although not significant, plasma membrane bound B_2 under GTPase-null dynamin 2 conditions was shown to increase 1.5-fold and 1.7-fold over cells transfected with wild type dynamin 2 or the empty vector alone, respectively (Fig. 5A). The enhanced enrichment of B_2 to the membrane surface was shown to be more pronounced under cotransfection conditions (i.e., DNM2 siRNA + $DNM2^{K44A}$), which led to 1.8-fold, 2-fold and 1.4-fold higher membrane localization when compared to the effects of wild type, the empty vector, and the cotransfection treatment involving non-targeting siRNA and the empty vector, respectively. A similar trend was noted for the control ligand, transferrin. Transient transfections involving GTPase-null dynamin 2 revealed nearly 2-fold and 2.4-fold higher TF localization at the plasma membrane versus the effects of wild type dynamin 2 and empty vector treatments, respectively (Fig. 5B). Similar to B_2, the cotransfection condition led to a more pronounced enrichment of TF at the membrane surface that was 1.5-fold and nearly 3-fold higher than the effects of the negative control cotransfection treatment (i.e., N siRNA +

Molecular Pharmacology Fast Forward. Published on June 12, 2007 as DOI: 10.1124/mol.107.037101
This article has not been copyedited and formatted. The final version may differ from this version.

empty vector) and the empty vector, respectively. These results are in agreement with the data from cells transfected with DNM2 pool siRNA alone, and provide additional evidence that actively internalized B_2 requires, in part, the functional expression of the highly conserved mechanoenzyme, dynamin 2, for its endocytic translocation in human placental trophoblasts.

Rhodamine-Labeled-B_2 Colocalizes With the Caveolae Coat Protein, Caveolin 1. Caveolin 1 (CAV1) is characterized to function in caveolae-mediated endocytosis in mammalian cells (Pelkmans et al., 2004). Specifically, CAV1 is a cytoplasmically oriented integral membrane protein known to bind cholesterol (Uittenbogaard and Smart, 2000) and associates with cholesterol- and sphingolipid-rich plasma membrane domains termed caveolae. CAV1 is one of three known caveolin isoforms that has been characterized to be critical in signal transduction pathways, membrane organization, and ligand bound receptor mediated trafficking specific to CvME in many divergent cell systems (Cheng et al., 2006). Some of the classical ligands that have been characterized to be absorbed and trafficked via this pathway include cholera toxin subunit B and folate (Birn, 2006; Shajahan et al., 2004). Furthermore, like CME, CvME is dependent on dynamin 2 for vesicle formation and release from the plasma membrane (Yao et al., 2005).

Internalized rhodamine-B_2 (Rd-RF), AlexaFluor®555-labeled cholera toxin subunit B (CTX), or TAMRA-labeled TF were examined for colocalization with immunofluorescence detected endosome markers, CAV1 or clathrin, in BeWo cells. All fluorescence colocalization assessments were further analyzed for intact cell morphology using differential interference contrast imaging (data not shown). After a 2 min uptake period, both Rd-RF and CTX resulted in punctate staining resembling endosomal organelle localization (Fig. 6A). Similar to CTX, Rd-RF resulted in substantial overlap with CAV1. However, signal overlap between Rd-RF and CAV1 resulted in a largely peripheral cytoplasmic staining pattern compared to the perinuclear staining noted for colocalized CTX and CAV1 channels. In addition, Rd-RF and the positive control

Molecular Pharmacology Fast Forward. Published on June 12, 2007 as DOI: 10.1124/mol.107.037101
This article has not been copyedited and formatted. The final version may differ from this version.

ligand, transferrin, revealed punctate, perinuclear signal overlap with clathrin-positive endosomes after this same time period (Fig. 6B).

With the objective of defining the degree of involvement of these distinct endocytic pathways in B_2 intracellular trafficking, the extent of colocalization between ligands and the endocytic markers was defined as the percent of the total detected ligand volumes (cubic μm) and represents 2 and 10 min internalization periods (Fig. 7A). Interestingly, Rd-RF revealed the greatest extent of colocalization at the 2 min time point, and resulted in a similar degree of overlap with both endocytic markers (20.77 ± 13.30% SEM for overlap with clathrin-vesicles and 34.40 ± 9.36% SEM for overlap with caveolin 1-vesicles). Likewise, TF revealed maximal clathrin-endosome localization for the shortest uptake period (26.05 ± 13.84% SEM). However, CTX revealed increasing ligand buildup to caveolin 1-positive endosomes with maximal colocalization after 10 min (39.16 ± 10.07% SEM). Combined, these data reveal B_2 trafficking along the clathrin-dependent and caveolae-mediated endocytic pathways occur simultaneously and to a similar extent. Furthermore, Rd-RF ligand buildup to caveolin 1-positive vesicles occurs at a faster rate than that for CTX, and may reflect the high nutrient demands for B_2 in normal cell growth and function in the placental trophoblast cell system. Overlapping fluorescence intensities between ligands and endosome markers were further examined for 3D shape similarities using the Pearson's Correlation (PC) statistical test (Manders et al., 1993). This test is commonly used to reveal linear relationships existing between colocalized objects. Values > 0.0 define positive overlap between fluorescent channels, whereas values of 0.0 or < 0.0 are interpreted as no- and negative correlations, respectively. Similar to the control ligands, Rd-RF revealed positive fluorescence signal overlap with both endocytic markers for both time points (Fig. 7B), and thus further suggests simultaneous ligand enrichment to these distinct endosomal populations. Interestingly, a nearly 2-fold higher PC value was defined for the 2 min uptake period versus the 10 min time point for Rd-RF overlap with clathrin. This is in agreement with prior reports that have defined the transient association of the clathrin coat proteins with

nascently formed endosomes from plasma membranes (Barouch et al., 1997). The initial stages of clathrin-mediated endocytosis from the time of ligand-bound-receptor recruitment to clathrin-coated pits at the plasma membrane to the budding and release of the early endosome have been revealed to take place within 1-2 min across different cell systems (Schmid, 2004). Immediately following this time, the clathrin coat dissociates from the endosome surface and is free to re-associate along the cytoplasmic face of the plasma membrane to recruit more ligand-bound receptors into the cell. The fact that we do not observe similar trends with the CME ligand, transferrin, may reflect a faster rate of ligand internalization and recycling that has been documented in prior reports (Dautry-Varsat et al., 1983) and may be more fully appreciated using real-time imaging methods. Unlike clathrin, caveolin 1 is an integral membrane protein coat that remains with newly formed endosomes from the cell surface. Therefore, the similar PC values revealed for both time points representing Rd-RF and CTX overlap with CAV1 would be expected. Overall, the data from these fluorescence colocalization studies suggest Rd-RF intracellular trafficking in human placental trophoblasts occurs simultaneously and to a similar extent through distinct endocytic pathways requiring clathrin and caveolin 1.

Molecular Pharmacology Fast Forward. Published on June 12, 2007 as DOI: 10.1124/mol.107.037101
This article has not been copyedited and formatted. The final version may differ from this version.

Discussion

A dual approach involving RNAi and wild-type or dominant-negative plasmid transfections was carried out to delineate the involvement of the conserved endocytic mechanoenzyme, dynamin 2, in B_2 absorption in the human placental trophoblast model, BeWo. We showed that the endocytosis of B_2 is regulated, in part, by the functional expression of dynamin 2 GTPase. The extent of dynamin 2 dependence in regulating cellular B_2 levels was similar to that of the clathrin-dependent RME ligand, transferrin. Attenuated internalization of both B_2 and TF (~ 60 and 70% of control conditions, respectively) correlated with ~ 80% reduced dynamin 2 levels. Thus, at least 50% of actively absorbed B_2 is estimated to involve a dynamin 2-dependent RME process. In addition, reductions in ligand uptake under these same conditions revealed a concomitant increase in B_2 and TF binding along the cell surface. In further support of the siRNA treatments alone, cotransfection results involving the GTPase-null dynamin 2 expression construct and DNM2 pool siRNA generated an amplified effect on the predominant ligand accumulation at the plasma membrane for both ligands. Although a B_2 specific receptor and the proposed B_2 soluble carrier protein remain to be identified, this data provides the most substantial evidence to date supporting the existence of such molecular machinery in humans.

Transferrin uptake in BeWo cells under silenced dynamin 2 protein expression is less pronounced as compared to other reports (Hinrichsen et al., 2003; Huang et al., 2004); however, this observation may be cell-type and transfection reagent specific. For instance, Huang and coworkers (Huang et al., 2004) revealed ~ 70-80% inhibition in transferrin absorption in HeLa cells that were transfected twice with siRNA targeting the clathrin heavy chain, i.e., a major protein component required in clathrin polyhedral lattice formation, or dynamin 2. However, two consecutive transfections using the DNM2 pool siRNA treatments in BeWo cells drastically attenuated cell growth and compromised cell morphology when

examined under light microscopy (data not shown). In another study by Soulet and colleagues (Soulet et al., 2005), a single siRNA transfection in HeLa cells using siRNA targeting sorting nexin 9, a protein that binds and regulates dynamin 2 activity and clathrin-mediated endocytic efficiency, resulted in 45% reduction in transferrin absorption. These data are comparable to the effects we observed for this control ligand in BeWo cells treated with DNM2 pool siRNA (i.e., 30% reduced transferrin uptake). This close agreement between our results in BeWo and that of Soulet and coworkers' studies in HeLa suggest our RNAi strategies are specific and effective in eliciting functional effects on the trafficking of the control ligand, transferrin.

Our laboratory recently showed a clathrin-mediated endocytic component regulating riboflavin absorption and trafficking in divergent cell systems (D'Souza et al., 2006b; Huang et al., 2003; Huang and Swaan, 2000; Huang and Swaan, 2001). Based on our results that showed the requirement for dynamin 2 expression in directing B_2 cellular entry, and considering the pluripotent nature of this scission enzyme on regulating different RME mechanisms, the question remained as to whether multiple and distinct endocytic pathways were regulating intracellular B_2 trafficking. The caveolae-mediated endocytic mechanism is a candidate pathway that, like CME, requires dynamin 2 activity to allow for endocytic vesicle release of ligand-receptor cargo from the plasma membrane. Established fluorescent ligand endocytosis assays involving the characterized rhodamine-B_2 conjugate were carried out to define the extent of colocalized signal intensities with the immunofluorescence detected caveolar endosome marker protein, caveolin 1, and were compared to colocalization assessments between the B_2 conjugate and clathrin-positive vesicles. Three-dimensional confocal laser scanning microscopic analyses revealed similar extents in B_2 localization to both clathrin- and caveolin 1-positive vesicles after 2 and 10 min uptake periods. In addition to this vitamin's dependence on clathrin-mediated endocytosis, the intracellular distribution of absorbed B_2 in human epithelia is implicated to involve for the first time the caveolar mediated pathway.

Molecular Pharmacology Fast Forward. Published on June 12, 2007 as DOI: 10.1124/mol.107.037101
This article has not been copyedited and formatted. The final version may differ from this version.

The concept of multiple endocytic processes regulating the cellular trafficking of a single ligand is not unique to B_2. Evidence of this phenomenon has been demonstrated for folate, tumor growth factor beta (TGF-β), and cholera toxin subunit B (Birn, 2006; Di Guglielmo et al., 2003; Shajahan et al., 2004). Considering the importance of maintaining cellular B_2 levels required for normal growth and development, the existence of multiple cellular transport mechanisms would provide additional controls to meet such nutritional demands in states of physiological distress. In the case for TGF-β, Di Guglielmo and colleagues demonstrated a biochemical feedback mechanism regulating its internalization via either the clathrin-mediated or caveolar-mediated pathways (Di Guglielmo et al., 2003). Specifically, their data revealed the absorption of TGF-β along the CME pathway correlated with a signal transduction response as defined by interactions with the Smad anchor for receptor activation (SARA) protein. In contrast, caveolae-mediated endocytosis of TGF-β was coupled with the Smad7-Smurf2-dependent receptor degradation response and led to ubiquitin-dependent degradation of the TGF-β receptor. In this particular instance, the CvME mechanism appears to be involved in receptor degradation and ultimately receptor turnover, whereas the CME pathway functions in promoting signal transduction cascades. However, studies with epidermal growth factor (de Melker et al., 2001) have shown the CME pathway to facilitate receptor degradation through trafficking to lysosomal organelles. In the case for B_2, the involvement of two distinct RME pathways regulating its intracellular distribution may reflect a homeostatic mechanism of molecular sensors that either promote B_2-receptor activation coupled with increased vitamin endocytosis, or initiate receptor degradation and reduced ligand uptake.

In summary, the RNAi and dynamin 2 plasmid DNA transfection data provide definitive and direct evidence that a B_2 receptor-mediated endocytic mechanism exists in human placental trophoblasts. To date, dynamin 2 GTPase is the first protein identified in humans to serve as a regulator of B_2 cellular entry through RME. In addition to the clathrin-dependent B_2-RME

Molecular Pharmacology Fast Forward. Published on June 12, 2007 as DOI: 10.1124/mol.107.037101
This article has not been copyedited and formatted. The final version may differ from this version.

process, we report for the first time that B_2 trafficking involves the CvME pathway in the BeWo model. Understanding the cellular absorption and trafficking itineraries specific to B_2 will aid in future studies aimed at understanding various pathological states correlated with B_2-deficiency, and opens up novel drug targeting strategies that can be designed to bypass efflux transporters to potentially improve drug bioavailability. Conceptually and empirically, such drug formulations targeting either folate or transferrin RME pathways have been successfully demonstrated (Singh et al., 2006; Stephenson et al., 2003), and further promotes the feasibility of exploiting the B_2-RME portal as an alternative drug targeting route. Furthermore, recent reports (Rao et al., 2006; Rao et al., 1999) revealing substantially elevated serum riboflavin carrier protein (RCP) levels in breast and liver cancer patients compared to healthy subjects proposes a potential chemotherapeutic niche for such B_2-drug targeting initiatives.

Molecular Pharmacology Fast Forward. Published on June 12, 2007 as DOI: 10.1124/mol.107.037101
This article has not been copyedited and formatted. The final version may differ from this version.

Acknowledgments

We thank the laboratory of Dr. Mark A McNiven (Mayo Clinic and Foundation, Rochester, Minnesota) for graciously donating validated dynamin expression vectors. We also thank Dr. James I. Lee and Dr. Vanessa M. D'Souza for their valuable suggestions throughout this study.

References

Abrams VA, McGahan TJ, Rohrer JS, Bero AS and White HB, 3rd (1988) Riboflavin-binding protein from reptiles: a comparison with avian riboflavin-binding proteins. *Comp Biochem Physiol B* **90**:243-247.

Barouch W, Prasad K, Greene L and Eisenberg E (1997) Auxilin-induced interaction of the molecular chaperone Hsc70 with clathrin baskets. *Biochemistry* **36**:4303-4308.

Birn H (2006) The kidney in vitamin B12 and folate homeostasis: characterization of receptors for tubular uptake of vitamins and carrier proteins. *Am J Physiol Renal Physiol* **291**:F22-36.

Cao H, Garcia F and McNiven MA (1998) Differential distribution of dynamin isoforms in mammalian cells. *Mol Biol Cell* **9**:2595-2609.

Cao H, Orth JD, Chen J, Weller SG, Heuser JE and McNiven MA (2003) Cortactin is a component of clathrin-coated pits and participates in receptor-mediated endocytosis. *Mol Cell Biol* **23**:2162-2170.

Cheng ZJ, Singh RD, Marks DL and Pagano RE (2006) Membrane microdomains, caveolae, and caveolar endocytosis of sphingolipids. *Mol Membr Biol* **23**:101-110.

Conner SD and Schmid SL (2003) Regulated portals of entry into the cell. *Nature* **422**:37-44.

D'Souza VM, Bareford LM, Ray A and Swaan PW (2006a) Cytoskeletal scaffolds regulate riboflavin endocytosis and recycling in placental trophoblasts. *J Nutr Biochem* **17**:821-829.

D'Souza VM, Foraker AB, Free RB, Ray A, Shapiro PS and Swaan PW (2006b) cAMP-Coupled riboflavin trafficking in placental trophoblasts: a dynamic and ordered process. *Biochemistry* **45**:6095-6104.

Daniels TR, Delgado T, Helguera G and Penichet ML (2006) The transferrin receptor part II: targeted delivery of therapeutic agents into cancer cells. *Clin Immunol* **121**:159-176.

Dautry-Varsat A, Ciechanover A and Lodish HF (1983) pH and the recycling of transferrin during receptor-mediated endocytosis. *Proc. Natl. Acad. Sci. U. S. A.* **80**:2258-22562.

de Melker AA, van der Horst G, Calafat J, Jansen H and Borst J (2001) c-Cbl ubiquitinates the EGF receptor at the plasma membrane and remains receptor associated throughout the endocytic route. *J Cell Sci* **114**:2167-2178.

Di Guglielmo GM, Le Roy C, Goodfellow AF and Wrana JL (2003) Distinct endocytic pathways regulate TGF-beta receptor signalling and turnover. *Nat Cell Biol* **5**:410-421.

Fielding PE and Fielding CJ (1996) Intracellular transport of low density lipoprotein derived free cholesterol begins at clathrin-coated pits and terminates at cell surface caveolae. *Biochemistry* **35**:14932-14938.

Foraker AB, Khantwal CM and Swaan PW (2003) Current perspectives on the cellular uptake and trafficking of riboflavin. *Adv. Drug Deliv. Rev.* **55**:1467-1483.

Hill E, van der Kaay J, Downes CP and Smythe E (2001) The role of dynamin and its binding partners in coated pit invagination. *J Cell Biol* **152**:309-323.

Hinrichsen L, Harborth J, Andrees L, Weber K and Ungewickell EJ (2003) Effect of clathrin heavy chain- and alpha-adaptin-specific small inhibitory RNAs on endocytic accessory proteins and receptor trafficking in HeLa cells. *J Biol Chem* **278**:45160-45170.

Huang F, Khvorova A, Marshall W and Sorkin A (2004) Analysis of clathrin-mediated endocytosis of epidermal growth factor receptor by RNA interference. *J. Biol. Chem.* **279**:16657-16661.

Huang SN, Phelps MA and Swaan PW (2003) Involvement of endocytic organelles in the subcellular trafficking and localization of riboflavin. *J. Pharmacol. Exp. Ther.* **306**:681-687.

Huang SN and Swaan PW (2000) Involvement of a receptor-mediated component in cellular translocation of riboflavin. *J. Pharmacol. Exp. Ther.* **294**:117-125.

Huang SN and Swaan PW (2001) Riboflavin uptake in human trophoblast-derived BeWo cell monolayers: cellular translocation and regulatory mechanisms. *J. Pharmacol. Exp. Ther.* **298**:264-271.

Lamaze C, Baba T, Redelmeier TE and Schmid SL (1993) Recruitment of epidermal growth factor and transferrin receptors into coated pits in vitro: differing biochemical requirements. *Mol. Biol. Cell* **4**:715-727.

Manders MM, Verbeek PJ and Aten JA (1993) Measurement of co-localization of objects in dual colour confocal images. *J. Microscopy* **169**:375-382.

Mason CW, D'Souza VM, Bareford LM, Phelps MA, Ray A and Swaan PW (2006) Recognition, co-internalization, and recycling of an avian riboflavin carrier protein in human placental trophoblasts. *J. Pharmacol. Exp. Ther.* **317**:465-472.

McNiven MA, Cao H, Pitts KR and Yoon Y (2000) The dynamin family of mechanoenzymes: pinching in new places. *Trends Biochem. Sci.* **25**:115-120.

Pelkmans L, Burli T, Zerial M and Helenius A (2004) Caveolin-stabilized membrane domains as multifunctional transport and sorting devices in endocytic membrane traffic. *Cell* **118**:767-780.

Phelps MA, Foraker AB, Gao W, Dalton JT and Swaan PW (2004) A novel rhodamine-riboflavin conjugate probe exhibits distinct fluorescence resonance energy transfer that enables riboflavin trafficking and subcellular localization studies. *Mol. Pharm.* **1**:257-266.

Powers HJ (2003) Riboflavin (vitamin B-2) and health. *Am. J. Clin. Nutr.* **77**:1352-1360.

Powers HJ (2005) Interaction among folate, riboflavin, genotype, and cancer, with reference to colorectal and cervical cancer. *J. Nutr.* **135**:2960S-2966S.

Praefcke GJ and McMahon HT (2004) The dynamin superfamily: universal membrane tubulation and fission molecules? *Nat. Rev. Mol. Cell Biol.* **5**:133-147.

Querbes W, O'Hara BA, Williams G and Atwood WJ (2006) Invasion of host cells by JC virus identifies a novel role for caveolae in endosomal sorting of noncaveolar ligands. *J. Virol.* **80**:9402-9413.

Rao PN, Crippin J, Levine E, Hunt J, Baliga S, Balart L, Anthony L, Mulekar M and Raj MH (2006) Elevation of serum riboflavin carrier protein in hepatocellular carcinoma. *Hepatol. Res.* **35**:83-87.

Rao PN, Levine E, Myers MO, Prakash V, Watson J, Stolier A, Kopicko JJ, Kissinger P, Raj SG and Raj MH (1999) Elevation of serum riboflavin carrier protein in breast cancer. *Cancer Epidemiol Biomarkers Prev* **8**:985-990.

Said HM and Ma TY (1994) Mechanism of riboflavine uptake by Caco-2 human intestinal epithelial cells. *Am J Physiol* **266**:G15-21.

Schmid SL (2004) Endocytosis, in *Cell Biology* (Pollard TD, Earnshaw, WC ed) pp 355-367, Saunders, Elsevier, Inc., Philadelphia.

Shajahan AN, Timblin BK, Sandoval R, Tiruppathi C, Malik AB and Minshall RD (2004) Role of Src-induced dynamin-2 phosphorylation in caveolae-mediated endocytosis in endothelial cells. *J Biol Chem* **279**:20392-20400.

Sheff D (2004) Endosomes as a route for drug delivery in the real world. *Adv Drug Deliv Rev* **56**:927-930.

Singh M, Hawtrey A and Ariatti M (2006) Lipoplexes with biotinylated transferrin accessories: novel, targeted, serum-tolerant gene carriers. *Int J Pharm* **321**:124-137.

Soulet F, Yarar D, Leonard M and Schmid SL (2005) SNX9 regulates dynamin assembly and is required for efficient clathrin-mediated endocytosis. *Mol Biol Cell* **16**:2058-2067.

Stephenson SM, Yang W, Stevens PJ, Tjarks W, Barth RF and Lee RJ (2003) Folate receptor-targeted liposomes as possible delivery vehicles for boron neutron capture therapy. *Anticancer Res* **23**:3341-3345.

Uittenbogaard A and Smart EJ (2000) Palmitoylation of caveolin-1 is required for cholesterol binding, chaperone complex formation, and rapid transport of cholesterol to caveolae. *J Biol Chem* **275**:25595-25599.

van der Ende A, du Maine A, Simmons CF, Schwartz AL and Strous GJ (1987) Iron metabolism in BeWo chorion carcinoma cells. Transferrin-mediated uptake and release of iron. *J. Biol. Chem.* **262**:8910-8916.

Yao Q, Chen J, Cao H, Orth JD, McCaffery JM, Stan RV and McNiven MA (2005) Caveolin-1 interacts directly with dynamin-2. *J Mol Biol* **348**:491-501.

Zempleni J, Link G and Bitsch I (1995) Intrauterine vitamin B2 uptake of preterm and full-term infants. *Pediatr Res* **38**:585-591.

Zheng DB, Lim HM, Pene JJ and White HB, 3rd (1988) Chicken riboflavin-binding protein. cDNA sequence and homology with milk folate-binding protein. *J Biol Chem* **263**:11126-11129.

Molecular Pharmacology Fast Forward. Published on June 12, 2007 as DOI: 10.1124/mol.107.037101
This article has not been copyedited and formatted. The final version may differ from this version.

Footnotes page

a) Unnumbered footnote

This work was supported, in part, by the National Institutes of Health under grant DK56631 (to P. W. S.), a postdoctoral fellowship grant from the Susan G. Komen Foundation (to P.W.S.), and by a predoctoral fellowship sponsored by Eli Lilly and Company (to A. B. F.).

b) Send reprint requests to:

Peter W. Swaan, Ph.D., Department of Pharmaceutical Sciences, University of Maryland, 20 Penn Street, HSF2-621, Baltimore, MD 21201 USA; E-mail: pswaan@rx.umaryland.edu

c) Numbered Footnotes

Molecular Pharmacology Fast Forward. Published on June 12, 2007 as DOI: 10.1124/mol.107.037101
This article has not been copyedited and formatted. The final version may differ from this version.

Figure Legends

Fig. 1. Dynamin siRNA reveal target specific knockdown at the protein level. Cells transfected with duplex siRNA targeting mRNA for dynamin 2 (DNM2 pool), or dynamin-like protein 1 (DLP1) were examined for target protein knockdown using Western blotting and quantitative chemiluminescence-based densitometry, and normalized to housekeeping proteins, GAPDH or β-actin. Twenty and 40 nM targeting siRNA (A) DNM2p, and (B) DLP1 treatments were compared to 40 nM non-targeting (N) siRNA, mock, and untreated (U) cells. Cells treated with 40 nM targeting or non-targeting siRNA were assessed for the extent of DNM2 (C) or DLP1 (D) knockdown and were expressed as a percentage of non-targeting siRNA effects. The data represents the standard deviations of 2 to 4 separate experiments. Statistical significance between targeting and non-targeting effects on dynamin protein expression were defined by Student's *t*-test (**p<0.01).

Fig. 2. Silenced dynamin 2 states result in a significant reduction in actively internalized B_2 in BeWo cells. Cells transfected 63-72 hours prior with 40 nM siRNA were dosed with 5 nM [^{3}H]-B_2 for 4 min at (A) 37 °C or (B) 4 °C. Actively internalized B_2 (uptake at 37 ˚C) was determined by subtracting passively absorbed riboflavin (uptake at 4 ˚C). This data represents the standard deviations of 3 to 5 separate experiments. Statistical significance between targeting and non-targeting treatments was defined using one-way ANOVA with Newman-Keuls multiple comparison test (*p < 0.05).

Fig. 3. To a similar extent as the control endocytic ligand, transferrin, riboflavin uptake was reduced exclusively under silenced dynamin 2 conditions. BeWo cells transfected 63-72 hours prior with 40 nM siRNA were dosed with either 5 nM [^{3}H]-B_2 or 10 nM ^{125}I-transferrin (TF) for 4 min at 37 °C or 4 °C. Both actively internalized (A) B_2 and (B) TF are significantly reduced

Molecular Pharmacology Fast Forward. Published on June 12, 2007 as DOI: 10.1124/mol.107.037101
This article has not been copyedited and formatted. The final version may differ from this version.

exclusively under DNM2 pool siRNA treatments. The results reflect the standard deviations of 4-6 separate experiments. Statistical significance between targeting siRNA and non-targeting treatments was defined using one-way ANOVA with Newman-Keuls multiple comparison test (*$p < 0.05$).

Fig. 4. SiRNA-induced silencing of dynamin 2 leads to ~ 3-fold higher B_2 enrichment to the plasma membrane. BeWo cells transfected with 40 nM duplex siRNA were used in uptake assays (63-72 hours post-transfection) to examine the extent of bound versus internalized ligand upon dosing cells for 4 min with either 5 nM [^{3}H]-B_2 or 10 nM ^{125}I-TF. Data analyses involved equations 1 and 2 defined under methods and materials for membrane associated and internalized B_2 (A) and TF (B). Ligand localization was further characterized for the overall extent of plasma membrane bound over internalized B_2 (C) and TF (D). These data represent the standard deviations of 3 to 8 separate experiments. Statistical significance between targeting and non-targeting effects on ligand distribution was determined using one-way ANOVA with Newman-Keuls multiple comparison test (*$p < 0.05$, ***$p < 0.001$).

Fig. 5. Over-expression of GTPase-null dynamin 2 results in enhanced ligand localization at the plasma membrane. BeWo cells were transiently transfected with 400 ng each of either wild type dynamin 2 (DNM2^{WT})**,** GTPase-null dynamin 2 (DNM2^{K44A}), or with a combination of DNM2^{K44A} and 40 nM DNM2 pool siRNA. Sixty three to 72 hours post-transfection, cells were dosed with 5 nM [^{3}H]-B_2 or 10 nM ^{125}I-TF for 4 min at 37 ˚C, and examined for membrane associated and internalized ligands. Ratios were defined for plasma membrane bound over internalized (A) B_2 and (B) TF. The effects of dynamin 2 expression vectors or GTPase-null dynamin 2 cotransfections with DNM2 siRNA on ligand localization were defined through comparisons to single transfections with an empty vector or empty vector cotransfections with 40 nM non-targeting siRNA (N siRNA), respectively. These data represent the standard deviations of 3-4

separate experiments. Statistical significance between experimental treatments and control conditions were determined using one-way ANOVA with Newman-Keuls multiple comparison test (*$p < 0.05$, **$p < 0.01$).

Fig. 6. Rhodamine-riboflavin (Rd-RF) colocalizes with the caveolae coat protein, caveolin 1 (CAV1) and clathrin after 2 min uptake in BeWo cells. Rd-RF and positive control ligands, cholera toxin subunit B (CTX; ligand of CvME) and transferrin (TF; ligand of CME), were examined for colocalization with the immunostained endocytic protein markers, (A) CAV1 or (B) clathrin, after ligand internalization in BeWo cells for 2 min. Images represent 3D orthogonal profiles with the inset view defining the XY plane, and the outer panels reveal the YZ (right narrow panel) and XZ (top narrow panel) focal planes. Fluorescence signals for each channel were merged to reveal regions of colocalization (indicated by arrows and yellow regions). Scale bars (10 μm) are shown in the lower left corner of the merged XY panel. All images were acquired using 120x magnification.

Fig. 7. Rd-RF colocalizes with caveolin 1-positive endosomes to a similar extent as with clathrin-positive vesicles. (A) Overlapping (i.e., colocalized) volumes (cubic μm) for ligands and endosome marker channels were expressed as a percentage of the total volume for each ligand, and represent the mean ± the standard error of the mean for 3-4 regions of interest. (B) The Pearson's Correlation (PC) was chosen to define the likeness in 3D shapes between overlapping ligand and vesicle marker channels. A positive value for PC reflects a positive correlation in fluorescence signal overlap. Data in this graph are expressed as the mean ± the standard deviation for 3-4 regions of interest.

Figure 1

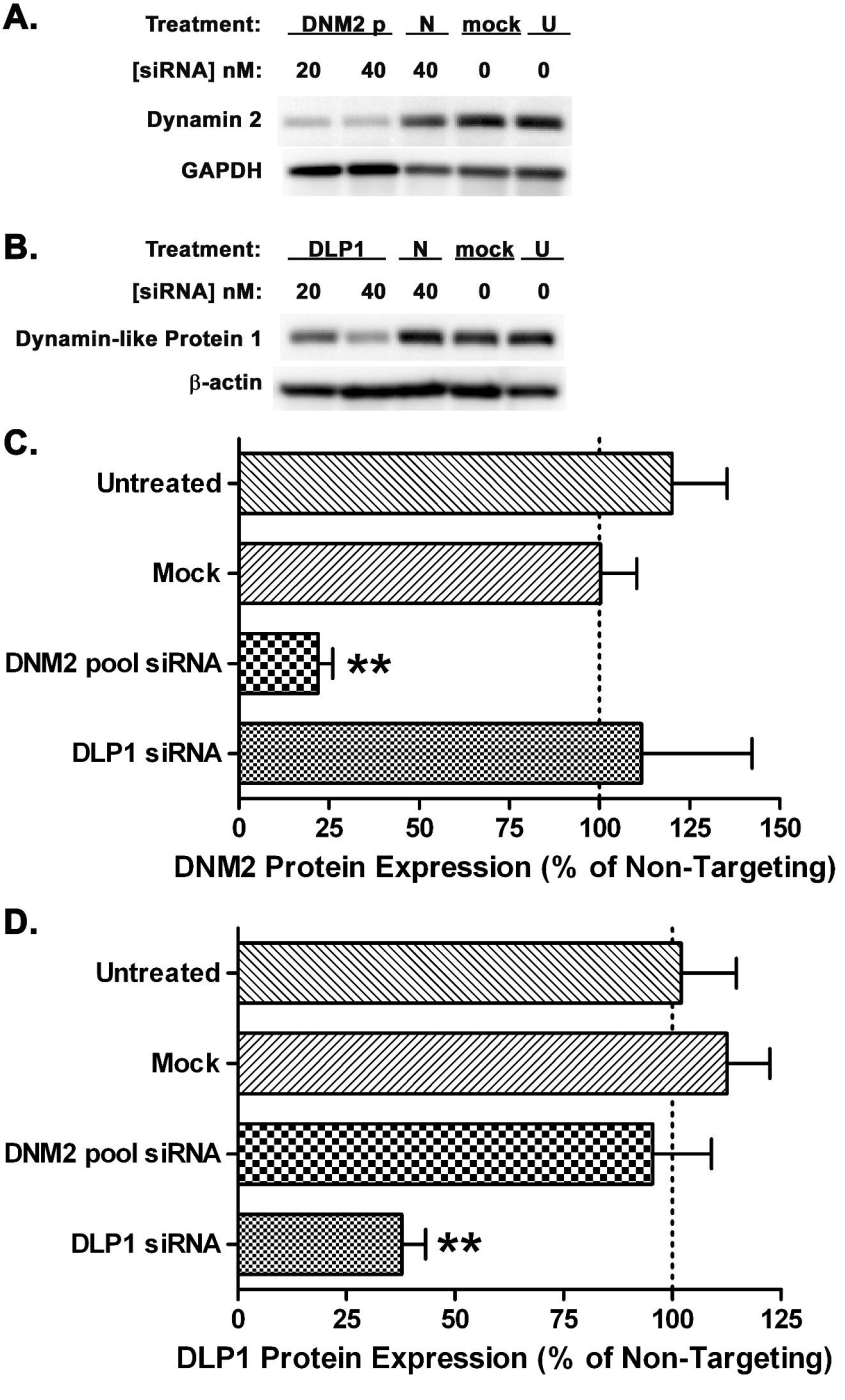
A.
Treatment: DNM2 p N mock U
[siRNA] nM: 20 40 40 0 0
Dynamin 2
GAPDH
B.
Treatment: DLP1 N mock U
[siRNA] nM: 20 40 40 0 0
Dynamin-like Protein 1
β-actin
C.
Untreated
Mock
DNM2 pool siRNA
DLP1 siRNA
**
0 25 50 75 100 125 150
DNM2 Protein Expression (% of Non-Targeting)
D.
Untreated
Mock
DNM2 pool siRNA
DLP1 siRNA
**
0 25 50 75 100 125
DLP1 Protein Expression (% of Non-Targeting)

Figure 2

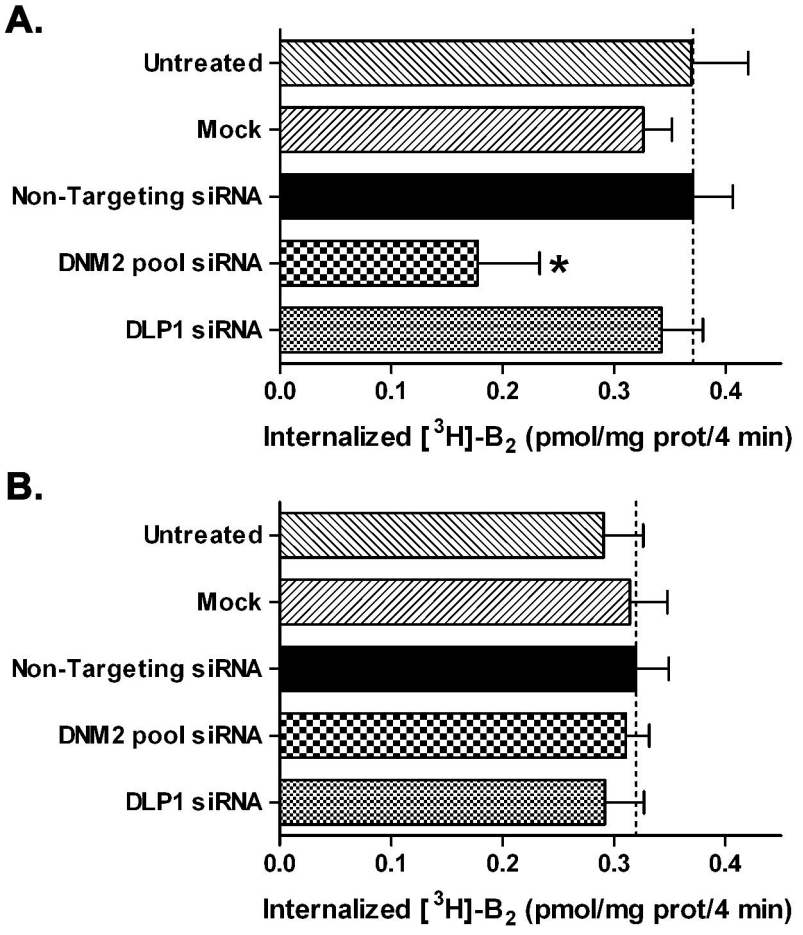
A.
Untreated
Mock
Non-Targeting siRNA
DNM2 pool siRNA
DLP1 siRNA
*
0.0
0.1
0.2
0.3
0.4
Internalized [3H]-B2 (pmol/mg prot/4 min)
B.
Untreated
Mock
Non-Targeting siRNA
DNM2 pool siRNA
DLP1 siRNA
0.0
0.1
0.2
0.3
0.4
Internalized [3H]-B2 (pmol/mg prot/4 min)

Figure 3

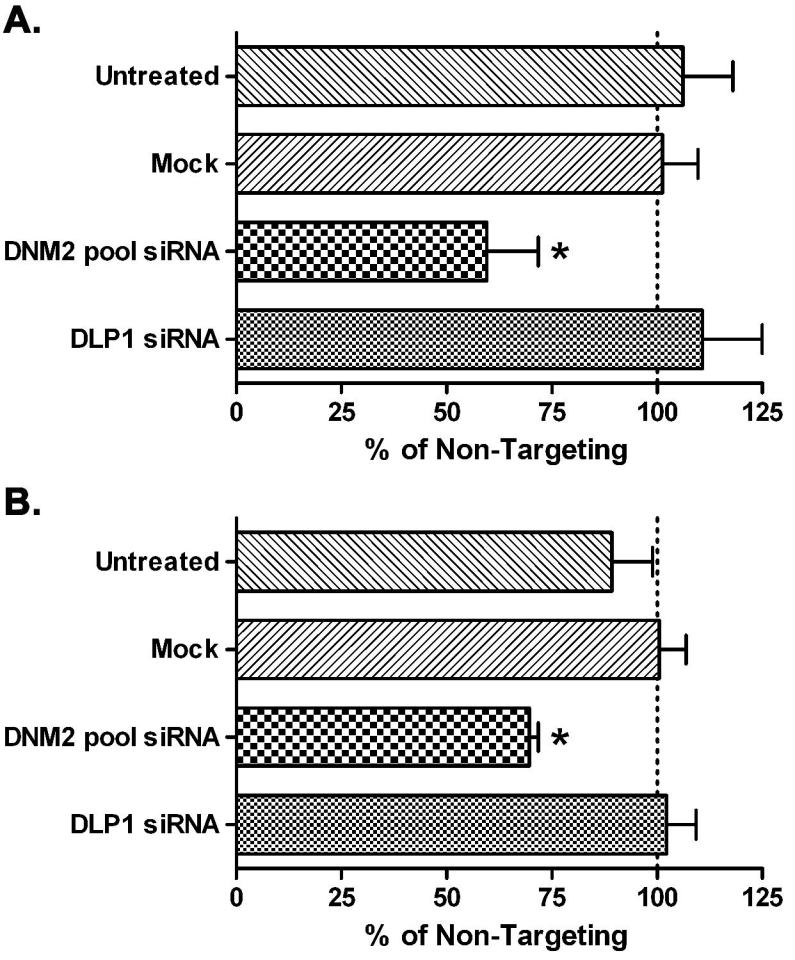
A.
Untreated
Mock
DNM2 pool siRNA
DLP1 siRNA
*
0
25
50
75
100
125
% of Non-Targeting
B.
Untreated
Mock
DNM2 pool siRNA
DLP1 siRNA
*
0
25
50
75
100
125
% of Non-Targeting

Figure 4

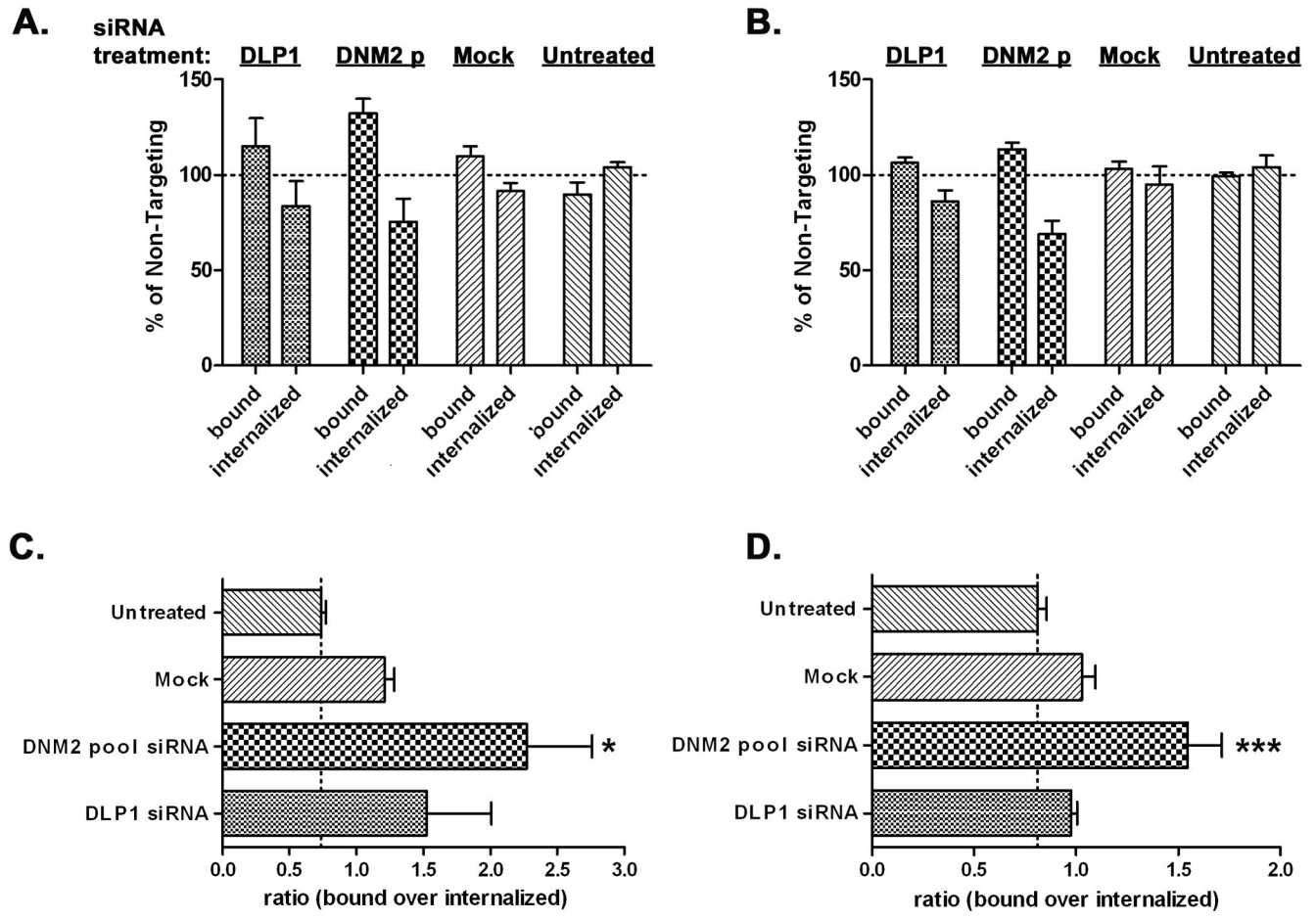
A.
siRNA treatment:
DLP1
DNM2 p
Mock
Untreated
% of Non-Targeting
150
100
50
0
bound
internalized
B.
C.
Untreated
Mock
DNM2 pool siRNA
DLP1 siRNA
*
0.0
0.5
1.0
1.5
2.0
2.5
3.0
ratio (bound over internalized)
D.
***

Figure 5

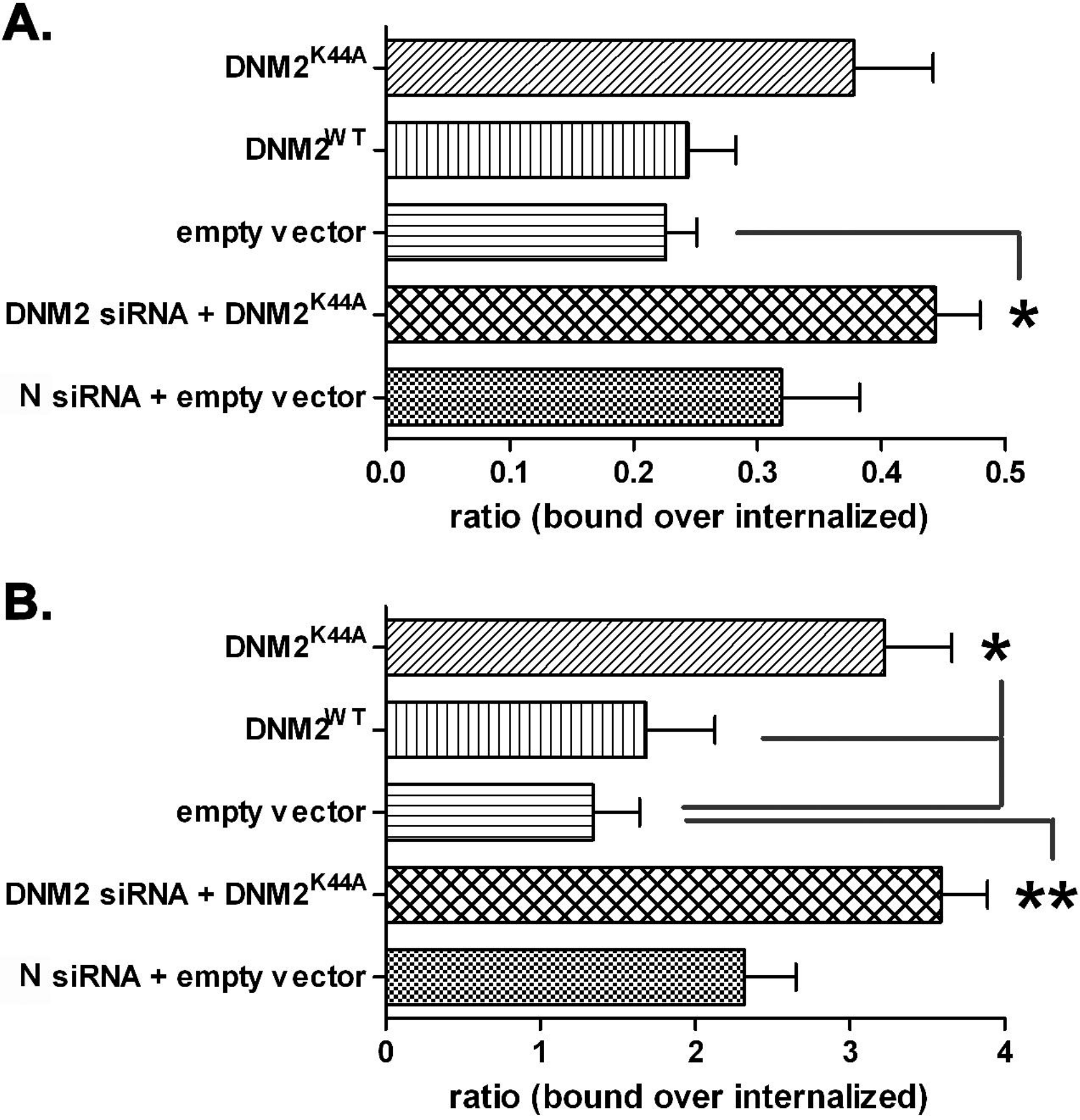
A.
DNM2K44A
DNM2WT
empty vector
DNM2 siRNA + DNM2K44A
N siRNA + empty vector
*
0.0
0.1
0.2
0.3
0.4
0.5
ratio (bound over internalized)
B.
DNM2K44A
DNM2WT
empty vector
DNM2 siRNA + DNM2K44A
N siRNA + empty vector
*
**
0
1
2
3
4
ratio (bound over internalized)

Figure 6

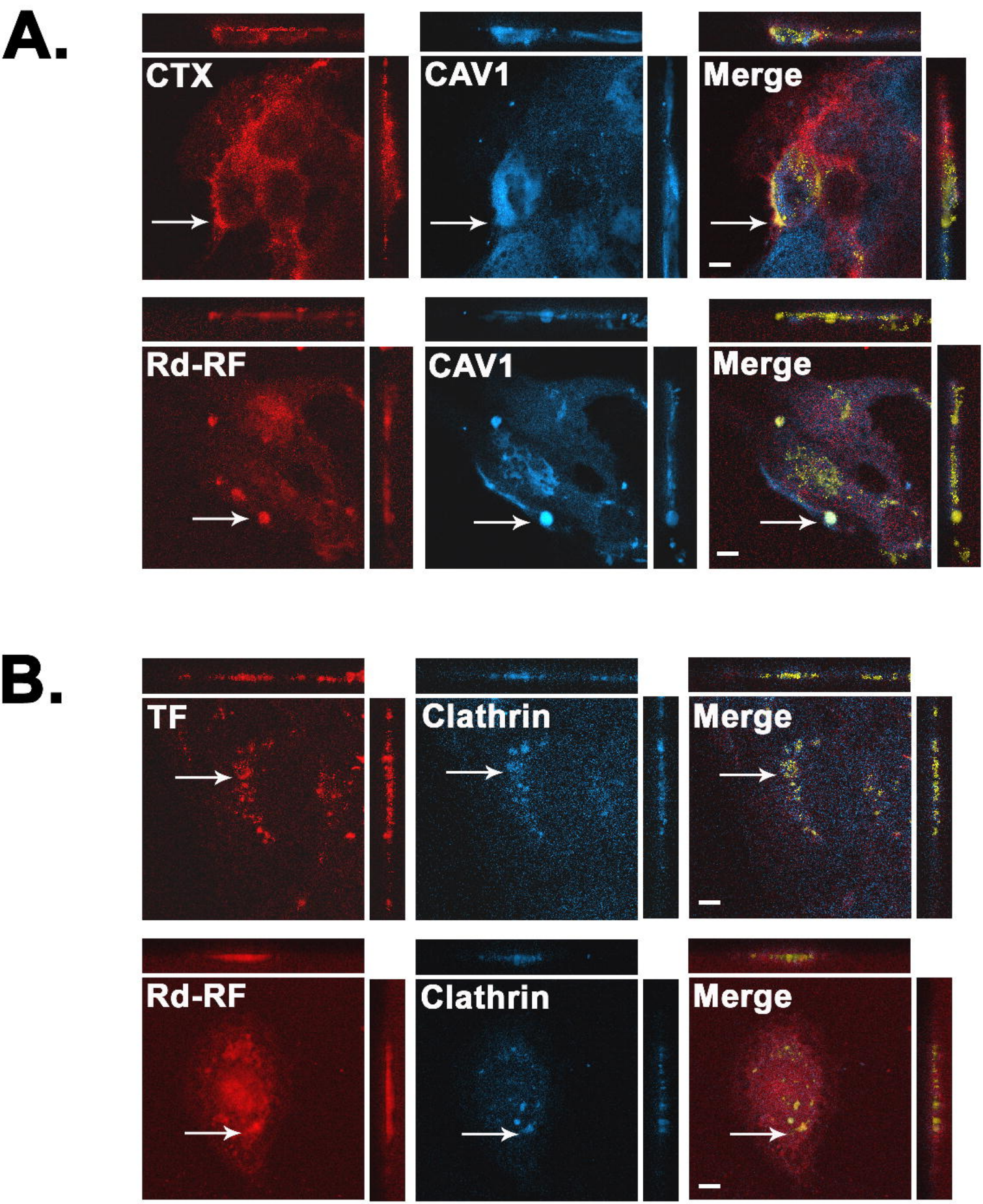
A.
CTX
CAV1
Merge
Rd-RF
CAV1
Merge
B.
TF
Clathrin
Merge
Rd-RF
Clathrin
Merge

Figure 7

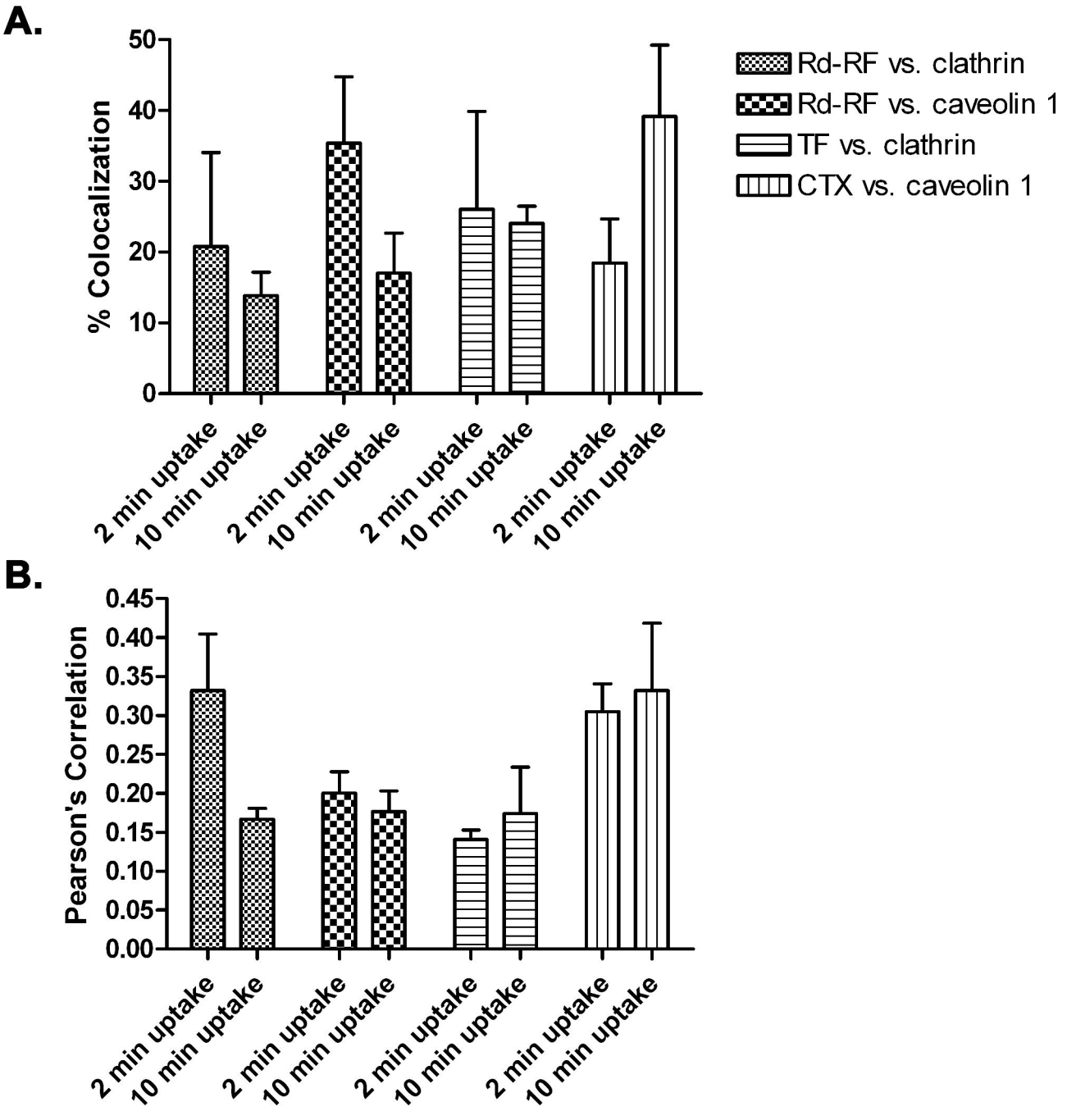
A.
% Colocalization
50
40
30
20
10
0
Rd-RF vs. clathrin
Rd-RF vs. caveolin 1
TF vs. clathrin
CTX vs. caveolin 1
2 min uptake
10 min uptake
B.
Pearson's Correlation
0.45
0.40
0.35
0.30
0.25
0.20
0.15
0.10
0.05
0.00